DOI: 10.6919/ICJE.202510\_11(10).0008

# Application of Predictive Control for Synchronous Motors in Oil Field Automation

Wendi Chu, Xinlong Shui

Eighth Oil Production Plant, Daqing Oilfield Co., Ltd., Daqing, Heilongjiang, 163400, China

## **Abstract**

For permanent magnet synchronous motor (PMSM) systems exhibiting strong coupling, parameter uncertainties, and dynamic load disturbances, this paper proposes a Model-Free Adaptive Control with Multi-Vector Predictive Current Control (MFAC-MPCC) framework, integrating Compact Form Dynamic Linearization MFAC (CFDL-MFAC) for the speed loop and triple-vector model predictive current control (MPCC) for the current loop. The hybrid architecture decouples adaptive speed regulation from high-precision current tracking, achieving robust performance without reliance on motor parameters. Key advantages include: (1) Model-free operation via CFDL-MFAC, dynamically linearizing the speed loop using only I/O data; (2) Enhanced disturbance rejection through real-time adaptive tuning; (3) Superior current tracking via triple-vector MPCC, minimizing steady-state errors and harmonic distortions. Simulation comparisons with traditional PI control and CFDL-MFAC approach validate the effectiveness and superiority of the proposed MFAC-MPCC scheme.

# **Keywords**

Oil Field Automation; Synchronous Motor; Triple-Vector MPCC; Speed Control.

#### 1. Introduction

The Permanent Magnet Synchronous Motor (PMSM), renowned for its exceptional characteristics including high efficiency, superior power density, and an extensive operational speed range, has become a cornerstone technology in demanding applications such as new energy vehicle propulsion systems, precision industrial servo drives, and aerospace actuation. Under the global imperative of the "dual-carbon" strategy and escalating requirements for intelligent manufacturing, PMSM control systems now face increasingly stringent demands for enhanced control precision, rapid dynamic response capabilities, and robust performance resilience against disturbances [1]. As an inherently strongly coupled, multivariable nonlinear system, the PMSM is highly susceptible to performance degradation from motor parameter drift, unpredictable load torque disturbances, and thermal effects during extended operation. These vulnerabilities starkly expose the limitations of traditional model-dependent speed control strategies, which often rely on precise mathematical models of the motor dynamics that are difficult to obtain accurately and maintain under harsh, variable operating conditions.

Conventional Proportional-Integral (PI) based speed controllers fundamentally struggle to handle the complex nonlinearities and inherent uncertainties within the PMSM system due to their linear control structure and fixed gain parameters. While more modern control methods have been proposed, many still exhibit insufficient adaptability to abrupt operational changes encountered in real-world scenarios. The novel MFAC-MPCC control framework proposed in [2] effectively addresses these critical challenges through a strategically integrated dual-loop architecture. This architecture synergistically combines Compact Form Dynamic Linearization Model-Free Adaptive Control (CFDL-MFAC) for the outer speed regulation loop with a triple-vector based Model Predictive

DOI: 10.6919/ICJE.202510\_11(10).0008

Current Control (MPCC) strategy for the inner current control loop. The CFDL-MFAC component, leveraging dynamic input-output linearization principles as described in [3], enables truly model-free operation by reconstructing the system dynamics solely from real-time I/O data. This approach delivers three key advantages: (1) Complete independence from explicit PMSM parameters and mathematical models; (2) Real-time adaptive suppression of both internal uncertainties and external disturbances without requiring pre-defined disturbance models; and (3) Inherently low computational overhead, making it highly suitable for implementation on embedded microcontroller platforms commonly used in motor drives. Complementing this, the inner loop's triple-vector MPCC significantly enhances steady-state current tracking accuracy while simultaneously improving dynamic response performance compared to conventional single-vector approaches. By synergistically integrating adaptive, model-free speed regulation with high-precision, fast-response predictive current control, the MFAC-MPCC framework achieves demonstrably robust performance across a wide operating envelope, effectively handling variable load torques and significant motor parameter uncertainties, thereby outperforming both traditional PI controllers and many existing model-based control approaches in demanding applications.

# 2. Mathematical Model of a Permanent Magnet Synchronous Motor

This article is based on a surface-mounted PMSM (SPMSM), whose dq-axis inductances are equal. The vector control strategy of  $i_d^* = 0$  can be used to decouple PMSM. In the synchronous rotating dq reference frame, the torque model of PMSM can be described as:

$$u_{\rm d} = R_{\rm s}i_{\rm d} + L_{\rm d}\frac{di_{\rm d}}{dt} - \omega_{\rm re}\psi_{\rm q} \tag{1}$$

$$u_{q} = R_{s}i_{q} + L_{q}\frac{di_{q}}{dt} + \omega_{re}\psi_{d}$$
 (2)

$$\psi_{d} = L_{d}i_{d} + \psi_{f} \tag{3}$$

$$\psi_{\mathbf{q}} = L_{\mathbf{q}} i_{\mathbf{q}} \tag{4}$$

$$J\frac{d\omega}{dt} = T_e - T_L - B\omega \tag{5}$$

$$T_e = \frac{3}{2} p_n \left( \psi_{\rm d} i_{\rm q} - \psi_{\rm q} i_{\rm d} \right) \tag{6}$$

For a PMSM system, it can be decoupled by applying the vector control strategy with  $i_d^*=0$ . Thus, according to equations (3) to (4) and equation (6), the following electromagnetic torque equation can be obtained:

$$T_e = \frac{3}{2} p_n i_q \psi_f \tag{7}$$

Where:  $u_d$  and  $u_q$  are the d-axis and q-axis components of the stator voltage,  $R_s$  represents the stator resistance,  $i_d$  and  $i_q$  are the d-axis current and q-axis current,  $L_d$  and  $L_q$  are the d-axis component of

DOI: 10.6919/ICJE.202510\_11(10).0008

the stator inductance and q-axis component of stator inductance,  $\omega_{re}$  is the rotor electrical angular velocity,  $\psi_d$  and  $\psi_q$  are the d-axis component of the permanent magnet flux linkage and q-axis component of the permanent magnet flux linkage,  $\psi_f$  is the permanent magnet flux linkage, J is the moment of inertia, B is the damping coefficient,  $T_e$  is the electromagnetic torque,  $T_L$  is the load torque, and  $\omega$  is the mechanical angular velocity,  $p_n$  is the pole pair number of the motor.

Using equations (5) and (7), the continuous - time equation is discretized by the forward Euler method with a one - step approach.[4]:

$$\frac{\omega(k+1) - \omega(k)}{T_s} = \frac{3}{2J} p_n i_q(k) \psi_f - \frac{1}{J} T_L - \frac{B}{J} \omega(k)$$
(8)

Where:  $T_s$  is the sample period,  $\omega(k)$  is the speed control output of the system at moment k, and  $i_q(k)$  is the control current input of the system at moment k. Further rearrangement of equation (8) yields

$$\omega(k+1) = \left(1 - \frac{B}{J}T_s\right)\omega(k) + \frac{3}{2J}T_s p_n i_q(k)\psi_f$$

$$-\frac{1}{J}T_s T_L$$
(9)

The state equations for the d-axis current  $i_d$  and q-axis current  $i_q$  are as follows:

$$\frac{di_{\rm d}}{dt} = \frac{1}{L_{\rm s}} \left[ u_{\rm d} - R_{\rm s}i_{\rm d} + \omega_{\rm re}L_{\rm s}i_{\rm q} \right] \tag{10}$$

$$\frac{di_{\rm q}}{dt} = \frac{1}{L_{\rm s}} \left[ u_{\rm q} - R_{\rm s} i_{\rm q} - \omega_{\rm re} L_{\rm s} i_{\rm d} - \omega_{\rm re} \psi_{\rm f} \right]$$
(11)

Where:  $L_s$  denotes the stator inductance.

To calculate the predicted current value at the next sampling instant, the discrete prediction formulas for the d- and q-axis currents can be approximately derived using the Euler method as follows:

$$i_{d}(k+1) = \frac{T_{s}}{L_{s}} \left[ u_{d}(k) - R_{s}i_{d}(k) + E_{d}(k) \right]$$

$$+ i_{d}(k)$$

$$(12)$$

$$i_{q}(k+1) = \frac{T_{s}}{L_{s}} \left[ u_{q}(k) - R_{s}i_{q}(k) + E_{q}(k) \right] + i_{q}(k)$$
(13)

$$E_{\rm d}(k) = \omega_{\rm re}(k) L_{\rm s} i_{\rm q}(k) \tag{14}$$

DOI: 10.6919/ICJE.202510\_11(10).0008

$$E_{\rm q}(k) = -\omega_{\rm re}(k)L_{\rm s}i_{\rm d}(k) - \omega_{\rm re}(k)\psi_{\rm f}$$

$$\tag{15}$$

Where:  $i_d(k+1)$  and  $i_q(k+1)$  represent the predicted d-axis and q-axis currents at the next sampling instant, respectively;  $E_d(k)$  and  $E_q(k)$  are the d-axis and q-axis back electromotive forces (back-EMF) at the current instant, respectively;  $u_d(k)$  and  $u_q(k)$  are the d-axis and q-axis voltages at the current instant, respectively.

# 3. Speed Loop and Current Loop Design

#### 3.1 Traditional Model Predictive Current Control Current Control

Traditional Model Predictive Current Control (T-MPCC) replaces the two current inner loops of vector control with a model predictive controller, retaining only a speed loop PI controller, thus eliminating the need for complicated PI parameter tuning. In the T-MPCC control strategy, equation (12) and equation (13) are used to calculate the predicted values of d-axis and q-axis currents corresponding to seven basic voltage vectors respectively, and then these predicted values are substituted into the cost function of equation (16). The voltage vector that minimizes the cost function is selected as the optimal voltage vector and output to the inverter. In T-MPCC, the candidate vectors are seven voltage vectors with invariable directions and magnitudes.

$$g = |i_{q}^{*} - i_{q}(k+1)| + |i_{d}^{*} - i_{d}(k+1)|$$
(16)

Where:  $i_d^*$  is the reference value of the d-axis component of the stator current;  $i_q^*$  is the reference value of the q-axis component of the stator current.

## 3.2 Optimal Duty Cycle Model Predictive Current Control

Optimal Duty Cycle Model Predictive Current Control (ODC-MPCC) is an enhanced strategy based on T-MPCC that incorporates duty cycle modulation. It pre-calculates the duty cycles for all six active voltage vectors, then optimizes the pairing of an active voltage vector and its duty cycle using a cost function. In ODC-MPCC, the candidate vectors consist of six voltage vectors with fixed directions and adjustable magnitudes.

To achieve deadbeat control of the q-axis current, the q-axis current expression can be formulated as:

$$i_{q}(k+1) = i_{q}(k) + s_{i}\gamma_{i}T_{s} + s_{0}(T_{s} - \gamma_{i}T_{s}) = i_{q}^{*}$$
(17)

Where,  $\gamma_i$  denotes the duty cycle of the active voltage vector,  $s_0$  represents the slope of the q-axis current during zero-voltage vector application, and  $s_i$  indicates the slope of the q-axis current during active voltage vector, where the subscript i=1, 2, ..., 6 corresponds to the six active switching states in the context of three-phase inverter control.

$$s_0 = \frac{dq}{dt}\bigg|_{u_*=0} \tag{18}$$

$$s_{i} = \frac{dq}{dt}\Big|_{u_{0} = u_{0i}} = s_{0} + \frac{u_{qi}}{L_{s}}$$
 (19)

DOI: 10.6919/ICJE.202510\_11(10).0008

Where:  $u_{qi}$  denotes the q-axis component of the stator voltage corresponding to the *i*-th voltage vector. Accordingly, the duty cycle  $\gamma_i$  for the active voltage vector can be derived from Equation (17) as:

$$\gamma_{i} = \frac{i_{q}^{*} - i_{q}(k) - s_{0}T_{s}}{T_{s}(s_{i} - s_{0})}$$
(20)

Where,  $\gamma_i \in [0, 1]$ . The active time of the effective voltage vector is  $\gamma_i T_s$ , and the active time of the zero vector is  $(T_s - \gamma_i T_s)$ .

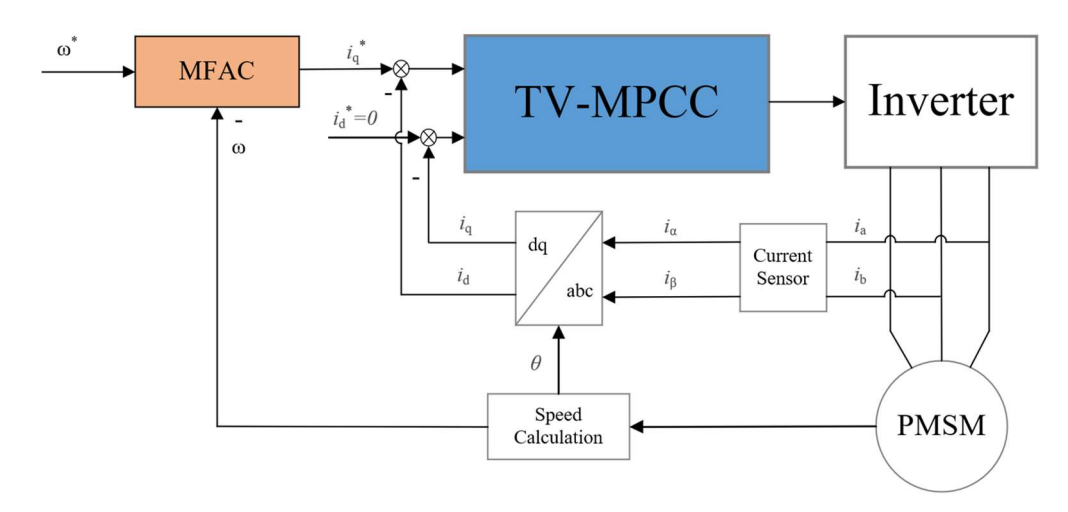


Figure 1. Control block diagram of MFAC-MPCC

#### 3.3 Three-Vector Model Predictive Current Control

Three-Vector-based Model Predictive Current Control (TV-MPCC) synthesizes a desired voltage vector in each sector by equivalently combining two adjacent active voltage vectors and one zero vector. Based on(10)(11), the formulas for the current slopes ( $s_{d(0,i,j)}$ ,  $s_{q(0,i,j)}$ ) under voltage vectors application as follows[5]:

$$s_{d0} = \frac{di_{d}}{dt}\Big|_{u_{s}=0} = \frac{1}{L_{s}} \left[ -R_{s}i_{d} + \omega_{re}L_{s}i_{q} \right]$$

$$(21)$$

$$s_{q0} = \frac{di_{q}}{dt}\bigg|_{u_{s}=0} = \frac{1}{L_{s}} \left[ -R_{s}i_{q} - \omega_{re}L_{s}i_{d} - \omega_{re}\psi_{f} \right]$$
(22)

$$s_{di} = \frac{di_{d}}{dt} \bigg|_{u_{d} = u_{di}} = s_{d0} + \frac{u_{di}}{L_{s}}$$
 (23)

$$s_{qi} = \frac{di_{q}}{dt}\bigg|_{u_{q} = u_{qi}} = s_{q0} + \frac{u_{qi}}{L_{s}}$$
 (24)

$$s_{dj} = \frac{di_{d}}{dt}\Big|_{u_{d} = u_{di}} = s_{d0} + \frac{u_{dj}}{L_{s}}$$
 (25)

DOI: 10.6919/ICJE.202510\_11(10).0008

$$s_{qj} = \frac{di_{q}}{dt}\bigg|_{u_{q} = u_{qj}} = s_{q0} + \frac{u_{qj}}{L_{s}}$$
 (26)

The predictive equations for the  $i_d$  and  $i_q$  currents can be formulated as follows:

$$i_{d}(k+1) = i_{d}(k) + s_{di}t_{i} + s_{di}t_{i} + s_{d0}t_{z} = i_{d}^{*}$$
(27)

$$i_{q}(k+1) = i_{q}(k) + s_{di}t_{i} + s_{qi}t_{j} + s_{q0}t_{z} = i_{q}^{*}$$
(28)

$$T_{s} = t_{i} + t_{j} + t_{z} \tag{29}$$

After calculating  $t_i$ ,  $t_j$ ,  $t_z$ , it is essential to verify whether they fall within the valid range  $[0, T_s]$ . If any value lies outside this interval, the application of its corresponding voltage vector must be canceled. The handling logic is classified as follows:

- 1) If  $t_z$  is not within the range  $[0, T_s]$ , but both  $t_i$  and  $t_j$  are within the range  $[0, T_s]$ , then two effective voltage vectors act during one control period.
- 2) If  $t_z$  is within the range  $[0, T_s]$  and only one of  $t_i$  or  $t_j$  is within the range  $[0, T_s]$ , then one effective voltage vector and the zero vector act during one control period.
- 3) If  $t_z$  is not within the range  $[0, T_s]$  and only one of  $t_i$  or  $t_j$  is within the range  $[0, T_s]$ , then one effective voltage vector acts throughout the entire control period.

Based on the proximity principle, the desired voltage vector is synthesized using two adjacent active voltage vectors and one zero vector, with the zero vector selected to minimize switching losses. Only one desired voltage vector needs to be synthesized per sector, resulting in six desired voltage vectors across all sectors. Since only six desired voltage vectors exist, merely six online predictions are required to select the optimal voltage vector.

When calculating the desired voltage vector, the dwell times  $t_i$ ,  $t_j$ , and  $t_z$  for two active voltage vectors  $(u_i, u_j)$  and one zero voltage vector are first determined. Subsequently, the d-axis and q-axis components of the desired voltage vector are computed using Equations (30) and (31), respectively.

$$u_{\rm d} = \frac{t_i}{T_{\rm s}} u_{\rm di} + \frac{t_j}{T_{\rm s}} u_{\rm dj} \tag{30}$$

$$u_{q} = \frac{t_{i}}{T_{s}} u_{qi} + \frac{t_{j}}{T_{s}} u_{qj} \tag{31}$$

After calculating  $t_i$ ,  $t_j$ ,  $t_z$ , it is essential to verify whether they fall with

The implementation procedure of the TV-MPCC strategy is as follows:

- 1) The sampled current values at the current sampling instant are obtained, calculating the current slopes according to Equations (21) to (26).
- 2) Select the basic voltage vectors and respectively calculate the operating times  $t_i$ ,  $t_j$ , and  $t_z$  of the three basic voltage vectors, then determine whether the calculated times meet the requirements.
- 3) Calculate the d-axis and q-axis voltage components of the six expected voltage vectors respectively using equations (30) and (31).

DOI: 10.6919/ICJE.202510\_11(10).0008

- 4) Substitute the calculated d-axis and q-axis voltage components of the six expected voltage vectors into equations (12) and (13) to get the predicted d-axis and q-axis current values corresponding to the six expected voltage vectors.
- 5) Substitute the predicted current values into equation (16), and select the expected voltage vector that minimizes the cost function g as the optimal vector  $u_{\text{out}}$  to apply to the inverter.

## 3.4 Compact Form Dynamic Linearization

Assumption 1: The partial derivative of  $\omega(k+1)$  in System (9) with respect to the control current input  $i_q(k)$  is continuous.

Assumption 2: System (9) satisfies the generalized Lipschitz condition: for any time k and when  $\Delta i_q(k) \neq 0$ , the following formula holds

$$|\Delta\omega(k)| \le b|\Delta i_a(k)| \tag{32}$$

Lemma 1: For the nonlinear system (32) satisfying Assumptions 1 and 2, when  $|\Delta iq(k)| \neq 0$ , there must exist a time-varying parameter  $\varphi(k) \in \mathbb{R}$ , known as the pseudo partial derivative (PPD), such that the system (32) can be transformed into the following CFDL data model[6,7]:

$$\Delta\omega(k+1) = \phi_c(k)\Delta i_a(k) \tag{33}$$

Where:  $\varphi(k)$  is a bounded time-varying parameter satisfying  $|\varphi(k)| \le b$ , and b > 0 is a constant.

The MFAC speed controller is designed based on the dynamic linearization data model. Consider the following controller input criterion function:

$$J[i(k)] = \left|\omega^*(k+1) - \omega(k+1)\right|^2 + \lambda \left|i(k) - i(k-1)\right|^2$$
(34)

Among them,  $\lambda > 0$  serves as a weighting factor, which is used to restrict the variation of the control input, Substitute equation (33) into equation (34), differentiate with respect to i(k), and set the derivative equal to zero.

$$i(k) = i(k-1) \frac{\rho \phi_c(k)}{\left|\phi_c(k)\right|^2 + \lambda} \left[\omega^*(k+1) - \omega(k)\right] + i(k-1)$$
(35)

Where:  $\rho$  is the step size factor  $\rho \in (0,1)$ .

Equation (35) contains the unknown pseudo-partial derivatives (PPD) $\varphi(k)$ , so it is necessary to consider their estimation algorithms. Consider the following estimation criterion function:

$$J\left[\phi_{c}(k)\right] = \left|\omega(k) - \omega(k-1) - \phi_{c}(k)\Delta i(k-1)\right|^{2} + \mu \left|\phi_{c}(k) - \phi_{c}(k-1)\right|^{2}$$

$$(36)$$

DOI: 10.6919/ICJE.202510\_11(10).0008

Where:  $\mu > 0$  is a weighting factor, used to penalize the large variations in the estimated values of  $PPD_{\phi}(k)$ .

Minimizing the criterion function (36), the estimation algorithm for PPD $\varphi(k)$  can be obtained:

$$\phi_{c}(k) = \phi_{c}(k-1) + \left[\Delta\omega(k) - \phi(k-1)\Delta i(k-1)\right]$$

$$*\frac{\eta \Delta i(k-1)}{\mu + \Delta i(k-1)^{2}}$$
(37)

Where:  $\eta \in (0, 1]$  is the step size factor. In order to enable the PPD estimation algorithm (37) to have the continuous estimation ability for time-varying parameters, the following reset algorithm is designed:

$$|\phi_{c}(k)| \leq \varepsilon \quad |\Delta i(k-1)| \leq \varepsilon$$

$$\cup sign(\phi_{c}(k)) \neq sign(\phi_{c}(1))$$
then  $\phi_{c}(k) = \phi_{c}(1)$ 
(38)

#### 3.5 System Stability Analysis

To demonstrate the convergence and stability of the designed motor speed control system, the speed controller was subject to the following assumptions.

Assumption 3: For any given bounded desired speed output signal  $\omega^*(k+1)$ , there always exists a bounded  $i_a^*(k)$  such that the system output driven by this control current input signal equals  $\omega^*(k+1)$ .

Assumption 3: For arbitrary time step k and  $\Delta i_q(k) \neq 0$ , the sign of the system's pseudo partial derivative remains invariant, it satisfies either  $\phi(k) > \varepsilon > 0$  or  $\phi(k) < -\varepsilon$ , where  $\varepsilon$  is a small positive constant.

Assumption 3 serves as a necessary condition for the solvability of the control problem, implying that system(9) is output controllable. Assumption 4 indicates that when the control current input increases, the output of the PMSM speed control system should be non-decreasing. This can be regarded as a quasi-linear characteristic of the system. Such a condition is analogous to the assumption in model-based control methods requiring the control direction to be known or at least invariant in sign.

Lemma 2:For the nonlinear system (9) satisfying Assumptions 1–4, when the desired speed  $\omega^*(k+1)=\omega^*=\text{const}$ , the MFAC-MPCC scheme guarantees that there exists a positive constant  $\lambda_{\min}>0$  such that for any  $\lambda>\lambda_{\min}$ :

1) The system's tracking error is convergent and satisfies

$$\lim_{k \to \infty} \left| \omega^* - \omega(k+1) \right| = 0$$

2) The input and output sequences of the system,  $\{i_q(k)\}\$  and  $\{\omega(k)\}\$ , are bounded.

**Table 1.** Motor model parameters

Parameter	R	$\Psi_{\!f}$	L	$p_n$	J	В
value	1.84 Ω	0.42 Wb	6.65 mH	4	0.002 kg·m²	0.008 N·m·s

DOI: 10.6919/ICJE.202510\_11(10).0008

ISSN: 2414-1895

$\mathbf{T}$	<b>T</b>	. 11 (	` .1	, 1	1
I ahia /	Parameter	table of	three	control	schemes
I abic 2.	1 arameter	table of	. инсс	COHUOI	SCHOILCS

	PI	CDFL-MFAC	MFAC-MPCC
Parameter	$K_{\rm P}$ =0.079 $K_{\rm I}$ =3.50	$\rho=1.0, \lambda=9.7, \eta=0.99, \mu=0.001, \\ \varepsilon=10-5, K_{P}=0.079, K_{I}=3.50$	$\rho$ =0.4, $\lambda$ =2, $\eta$ =0.99 $\mu$ =0.001, $\varepsilon$ =10-5
Initial value		$\varphi(1) = 1.1$	$\varphi(1) = 1.1$

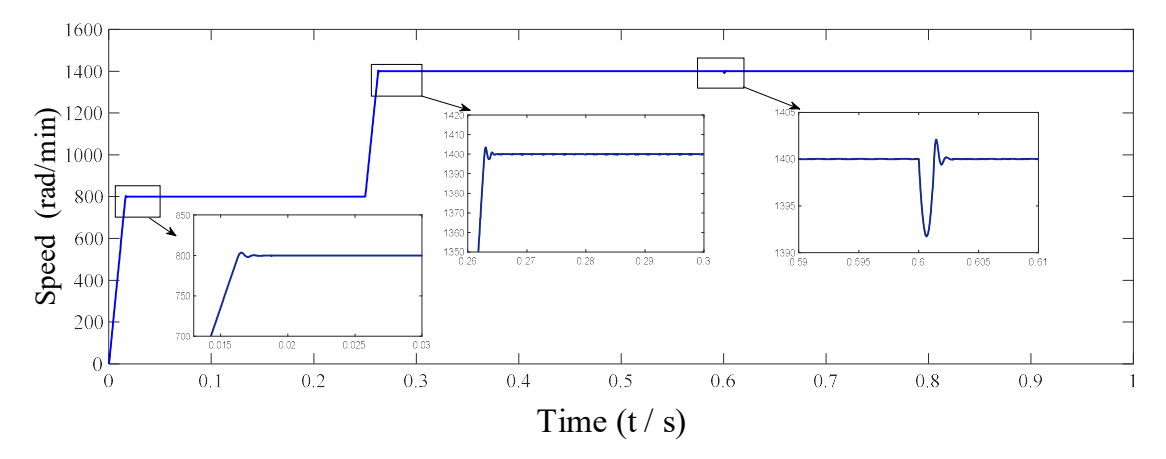


Figure 2. Motor speed output of MFAC-MPCC

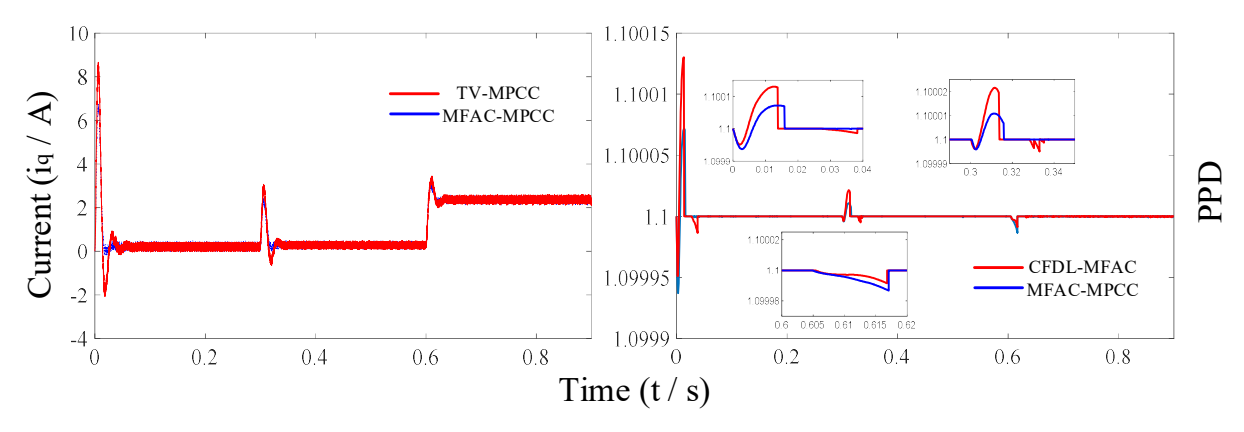


Figure 3. Comparative Analysis of Control Current and Pseudo Partial Derivative (PPD)

# 4. Simulation and Analysis

To validate the effectiveness and superiority of the proposed MFAC-MPCC scheme, this section carries out simulation verification on PMSM speed regulation utilizing MATLAB/Simulink. Comparative simulations are conducted against PI control, CFDL-MFAC, and MFAC-MPCC. The motor model parameters are carefully configured as detailed in Table 1.

Simulation duration = 0.9 s, DC-side voltage = 311 V, PWM switching frequency = 10 kHz. The reference speed is initially set to  $\omega^*$  = 800 rad/min. At t = 0.3 s, the reference speed increases to 1100 rad/min, followed by a torque of 10 N·m is applied at t=0.6 s. Parameters for the PI control, MFAC and MFAC-MPCC schemes are selected, as summarized in Table 2.

The speed output of the MFAC-MPCC is illustrated in Figures 2. Upon examination, it is evident that the proposed strategy exhibits outstanding performance, particularly in terms of rapid response capability and load disturbance rejection. When compared with TV-MPCC, the proposed control strategy achieves a notable reduction in current fluctuations, as demonstrated in Figure 3.

DOI: 10.6919/ICJE.202510\_11(10).0008

Additionally, in comparison with CFDL-MFAC, the pseudo partial derivative (PPD) displays smoother variations and enhanced adaptive performance.

## 5. Conclusion

MFAC-MPCC surpasses PI and conventional MPCC in PMSM control. MFAC-MPCC demonstrates superior control performance compared to both PI control and conventional MPCC control. It avoids reliance on motor models via an adaptive predictive framework, dynamically compensating nonlinearities with stable operation. Unlike MPCC's fixed parameters, it combines adaptive multistep optimization, improving transient response and current tracking accuracy. Its dual-loop structure effectively decouples speed-current dynamics and suppresses cross-coupling disturbances. In summary, MFAC-MPCC achieves higher control precision and anti-interference capability than PI and conventional MPCC, making it a promising solution for high-performance PMSM drives.

#### References

- [1] G. Eason, B. Noble, and I.N. Sneddon, "On certain integrals of Lipschitz-Hankel type involving products of Bessel functions," Phil. Trans. Roy. Soc. London, vol. A247, pp. 529-551, April 1955.
- [2] Y. Xu, J. Wang, B. Zhang, and Q. Zhou, "Three-vector model predictive current control for permanent magnet synchronous motor," Transactions of China Electrotechnical Society, vol. 33, no. 5, pp. 980–988, 2018 (in Chinese).
- [3] M. Yang, X. Lang, J. Long, and D. Xu, "Flux immunity robust predictive current control with incremental model and extended state observer for PMSM drive," IEEE Trans. Power Electron., vol. 32, no. 12, pp. 9267–9279, Dec. 2017.
- [4] R. Chi, Y. Hui, S. Zhang, B. Huang, and Z. Hou, "Discrete-time extended state observer-based model-free adaptive control via local dynamic linearization," IEEE Trans. Ind. Electron., vol. 67, no. 10, pp. 8691–8701, Oct. 2020.
- [5] Y. Wang and Z. Hou, "Model-free adaptive predictive control for PMSM systems with external disturbances," Control Theory & Applications, vol. 39, no. 5, pp. 837–846, May. 2022 (in Chinese).
- [6] Y. Xu, X. Ding, J. Wang, and Y. Li, "Three-vector-based low-complexity model predictive current control with reduced steady-state current error for permanent magnet synchronous motor," IET Electric Power Appl, vol. 14, no. 2, pp. 305–315, Feb. 2020.
- [7] C. Treesatayapun, "Equivalent Piecewise Derivative Adaptive Control With Fuzzy Rules Emulated Network and Mitigation of Catastrophic Forgetting Learning," IEEE Trans. Syst. Man Cybern, Syst., vol. 55, no. 1, pp. 758–767, Jan. 2025.